Annals of Nuclear Energy 165 (2022) 108646

Contents lists available at ScienceDirect

Annals of Nuclear Energy

journal homepage: www.elsevier.com/locate/anucene

Manufacturing LEU-foil annular target in Brazil

Michelangelo Durazzo *, Jose A.B. Souza, Ricardo F. Ianelli, Eriki M. Takara, Jose S. Garcia Neto, Adonis M. Saliba-Silva, Elita F. Urano de Carvalho

Nuclear and Energy Research Institute, IPEN-CNEN/SP, São Paulo, Brazil

A R T I C L E I N F O

Article history:
Received 26 March 2021
Received in revised form 3 August 2021
Accepted 15 August 2021

Keywords:
Annular target
Irradiation targets
Molybdenum-99
Uranium metal
Thin foil
Fabrication

A B S T R A C T

Molybdenum-99 is the most important isotope because its daughter isotope, technetium-99m, has been the most used medical radioisotope. The primary method used to produce Mo-99 derives from the fission of U-235 incorporated in so-called irradiation targets. Two routes are being developed to make Mo-99 by fissioning with low enriched uranium (LEU) fuel. The first adopts UAl_x-Al dispersion plate targets. The second uses uranium metal foil annular targets. The significant advantage of uranium foil targets over UAl_x-Al dispersion targets is the high density of uranium metal. This work presents the experience obtained in the development of the uranium metal annular target manufacturing steps. An innovative method to improve the procedure for assembling the uranium foil on the tubular target was presented. The experience attained will help the future production of Mo-99 in Brazil through the target irradiation in the Brazilian Multipurpose Reactor (RMB).

1. Introduction

The Nuclear Energy Agency (2016) reported in a review study that the radioactive isotope technetium-99m (Tc-99m) accounts for approximately 80% of all nuclear medicine procedures. Tc-99m is used in over 30 to 40 million medical diagnostic imaging procedures annually. Barnowski (2011) reported that technetium-99m is used in over 70 procedures to diagnose the severity of heart disease, track the spread of cancer, diagnose brain disease, and more applications are developed for its use every year. Tc-99m is derived from Mo-99, which is produced by nuclear fission of U-235 in research reactors. Uranium is incorporated into so-called irradiation targets, which are irradiated for about a week and then dissolved to extract Mo-99. Valuable information on the global production, use, and projected demand of Tc-99m is available in a report published by the U.S. National Academies of Sciences, Engineering, and Medicine (2016).

Because of the international supply crisis of Mo-99 that occurred in 2008–2009 (Ponsard, 2010; Verbeek, 2008) and the high dependence on external supply, the Brazilian government decided to build a new research reactor, mainly for domestic Mo-99 production. Obadia and Perrotta (2010) performed a sustainability analysis for implementing the new research reactor, which was based on several infrastructure issues suggested by the International Atomic Energy Agency (IAEA). This study concluded that the present national context and the established nuclear infrastructure favor implementing the new project, providing conditions for a sustainable life cycle for this new research reactor.

Perrotta and Soares (2014) describe the new research reactor's key characteristics, named the Brazilian Multipurpose Reactor (RMB). The reactor will be a 30 MW open pool-type reactor using LEU fuel (low enriched uranium fuel, <20 wt% U-235). The facility will be part of a new nuclear research center to be built about 100 km from São Paulo city in the southeast part of Brazil. Perrotta and Obadia (2011) provide information about the new research center, which will have several facilities. The targets needed to produce Mo-99 at the RMB research reactor are planned to be produced in Brazil.

Most Mo-99 producers employ high enriched uranium (HEU, 93 wt% U-235) in their production process, and non-proliferation initiative has required the removal of HEU from civilian nuclear facilities. In a review article, Hansell (2008) deals with the risks of nuclear terrorism associated with the Mo-99 production. To minimize the risk, since 1986, the US Reduced Enrichment for Research and Test Reactor Program (RERTR) has directed studies to replace the use of HEU with LEU targets (IAEA, 2015; Vandegrift et al., 1999). This level of enrichment prevents its use for nuclear bombs. International producers of Mo-99 are trying to replace conventional HEU targets with the LEU.

Conventional HEU targets are plate-type using U-Al alloy with uranium density of approximately 1.4 gU/cm^3. For maintaining the Mo-99 production level, the reduction of U-235 associated with the conversion from HEU to LEU had to be compensated by

* Corresponding author.
E-mail address: mdurazzo@ipen.br (M. Durazzo).

https://doi.org/10.1016/j.anucene.2021.108646
0306-4549/

increasing the uranium density of LEU targets. Kohut et al. (2000) developed an LEU target based on UAl_2 dispersion using a powder metallurgical route. In this process, uranium and aluminum metals are melted and cast into a UAl_2 ingot. The ingot of UAl_2 is then crushed into powder for the fabrication of UAl_2-Al dispersion plates according to the traditional technology based on the picture-frame technique. Kaufman (1962) first described this manufacturing technique, and Durazzo and Riella (2015) give detailed information about the picture-frame technique, which is extensively used for research reactor fuel production. Ali et al. (2013) describe the major procedures for manufacturing plate-type dispersion targets, and Mushtaq (2011) describes the qualification procedures.

For the fission-based production of Mo-99, the density (or loading) of U-235 per target is one of the most critical aspects of the target's design. Currently, the maximum uranium density of UAl_2 dispersion target plates is 2.6–2.7 gU/cm^3. Ryu et al. (2013) studied the experimental fabrication of dispersion target plates with 9 gU/cm^3 uranium density. The authors proposed using a centrifugal atomization technique to produce a high-content uranium alloy powder for its use in the dispersion with aluminum. Although this high uranium concentration has not yet been qualified under irradiation, this would theoretically be the maximum possible uranium loading on a plate-type target.

To increase efficiency in the production of Mo-99 by fission using LEU, the effort of the RERTR Program resulted in the development of an annular target using thin foils of low enriched uranium metal (Wiencek and Hofman, 1993; Conner et al., 1999). This new target has various advantages over the UAl_2-Al dispersion target. The uranium loading is the principal advantage. The LEU metal foil density is approximately 19 g/cm^3, much higher than the uranium loading of a typical LEU dispersion plate-type target. As a result, a uranium foil target can contain much higher uranium than the LEU plate-type target. Besides the advantage of the high uranium density in the annular foil target, Solbrekken et al. (2009) enumerated the following advantages: (1) the volume of radioactive liquid waste resulting from the chemical processing of uranium foil target is fifteen times smaller than the volume corresponding to the dispersion plate-type target (only uranium metal foil is dissolved); (2) the time required to dissolve a uranium foil target is less than that required to dissolve a dispersion plate-type target (only the metallic uranium foil is dissolved); (3) considering the mass of uranium contained in the target, the manufacturing cost of the uranium foil metal target is competitive with the manufacturing cost of the dispersion plate-type target.

The LEU annular targets are fabricated from hot- and cold-rolling of uranium metal to a thickness of around 125 μm. The uranium foil is wrapped in a 15 μm thick nickel foil which acts as a fission recoil barrier. The uranium/nickel foil is wound over the surface of an aluminum tube (inner tube), in which an undercut is machined where the uranium/nickel foil is positioned. The inner tube containing the uranium/nickel foil is inserted into another aluminum tube (outer tube). The assembled target is inserted in a draw die. It is consolidated by deforming the aluminum inner tube plastically by passing a draw plug with a slightly larger diameter than the inner tube's inner diameter. In this operation, the gaps between the tubes are eliminated (or reduced) to guarantee a good thermal contact that ensures the transfer of the heat generated in the uranium foil during the fission, getting the necessary cooling of the target. The nickel fission recoil barrier prevents the uranium foil from bonding to the aluminum tube cladding during irradiation. The target is then sealed by welding the ends to avoid contamination of the reactor environment by solid and gaseous fission during irradiation. Briyatmoko et al. (2007) provide an excellent overview of the annular target manufacturing process. The uranium foils are fabricated by hot-rolling. Wiencek et al. (2008) also studied the use of direct-cast foils. Vandegrift et al. (2016) provided complete information on the procedures for manufacturing annular uranium targets in an Argonne National Laboratory (ANL) report.

The cylindrical design was selected to improve the target structural integrity and heat transfer. Also, the design facilitates physical disassembly of the target after irradiation for Mo-99 recovery. After the target is irradiated, the uranium foil is recovered and chemically processed separately from the aluminum tubes. The separation of the uranium foil from the cladding before processing reduces the mass of material that must be chemically dissolved, advantageous to this target design. Brown et al. (2014) have developed two processes to dissolve these targets and recover Mo-99. For nitric acid dissolution, 98.4% Mo-99 was recovered. Targets electrochemically dissolved in an alkali carbonate media demonstrated over 92% Mo-99 recovery. These Mo-99 recovery yields are comparable with the recovery from UAl_x-Al dispersion targets, reported to be over 90% (Cols et al., 2000).

Wiencek et al. (2009) (Appendix A) presented an annular LEU foil target design developed by ANL. Based on this design, International Atomic Energy Agency (IAEA, 2018) offered to share the target manufacturing technology through the Coordinated Research Project (CRP) entitled "Developing Techniques for Small Scale Indigenous Molybdenum 99 Production Using Low Enriched Uranium (LEU) Fission or Neutron Activation". This CRP should allow participants to examine the feasibility of producing Mo-99 on a small-scale, using LEU-based fission Mo-99 production.

The Nuclear and Energy Research Institute (IPEN-CNEN/SP) has been fabricating fuel elements based on dispersion plate technology. For this reason, plate-type dispersion targets will be used in the first approach. However, the option of using annular targets containing uranium metal thin foil should not be ruled out because of its many advantages over plate targets. IPEN-CNEN/SP has also been fabricating uranium metal as raw material to produce the fuel elements for the IEA-R1 research reactor. Durazzo et al. (2017) describe the uranium metal fabrication at IPEN-CNEN/SP. The availability of uranium metal in Brazil encouraged the development of the annular foil target.

The uranium foil annular targets manufacturing steps were studied in this work, and the basic fabrication parameters were defined. An innovative method (and associated device) that facilitates the assembly of the uranium foil between the two concentric aluminum tubes have been used and is described. The manufacturing process showed to be suitable for the production of LEU annular targets.

2. Experimental

The main manufacturing steps of the annular uranium metal target are shown in Fig. 1. This work studied each of the steps for manufacturing this type of target.

2.1. Melting and casting uranium metal

IPEN-CNEN/SP has been producing low enriched uranium metal for many years. The production follows the route of UF_4 magnesiothermic reduction (Durazzo et al., 2017). In the present work, natural uranium metal was used.

Uranium metal was melted using an Indutherm 15 kW induction furnace (model VTC 200 V Ti) and cast in a graphite mold to get an ingot with 140 X 230 X 4 mm and 840 g. The melting crucible was made from magnesia-stabilized zirconia. The uranium metal was heated under an inert argon atmosphere at 1800 °C and poured into the graphite mold. The furnace was evacuated to

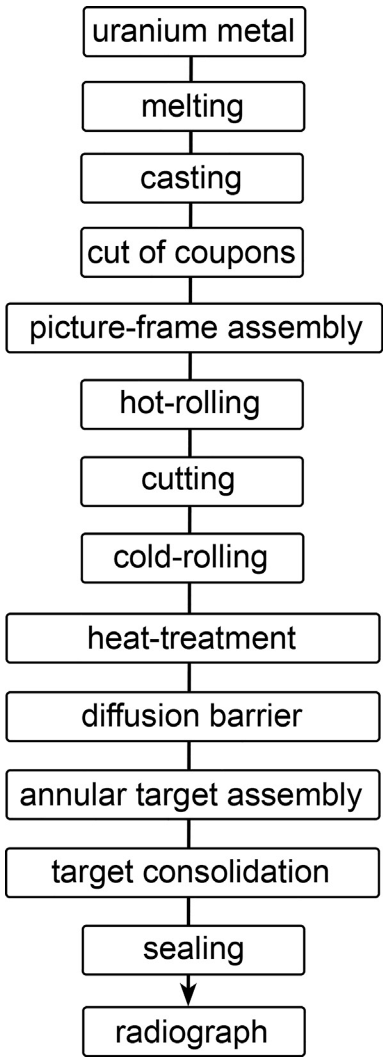

Fig. 1. Schematic of uranium foil annular target fabrication.

10^{-2} mbar and filled with ultra-pure argon. This operation was repeated three times.

Coupons 55 X 25 X 4 mm thick and mass around 96 g were cut out from the primary uranium metal ingot using a silicon carbide disc cutter. The key characteristics of the uranium metal produced are presented in Table 1.

2.2. Hot-rolling of coupons

The uranium metal coupon was hot-rolled using the picture-frame technique. The coupon was fitted into a hole machined in the center of a ‘‘picture frame” (23 cm X 12 cm X 0.4 cm) plate made of carbon steel. Two cladding plates with the same dimensions were assembled over and under the frame plate. The assembly components were manufactured with 1020 steel plates. Before assembly, the steel plates were sanded with 600 grit sandpaper until the surface was shiny. An aluminum-oxide/alcohol slurry with a thin paste consistency was applied over the frame and cladding plates to prevent bonding between uranium metal coupon and cladding steel plates during hot-rolling. The surface of the uranium coupon was also covered with Al_2O_3 slurry. Fig. 2 illustrates the assembly scheme of the coupon-frame-cladding as a sandwich.

The assembly was TIG (tungsten inert gas) welded (200 A), preparing for hot-rolling. Copper chill blocks were used to minimize the uranium metal coupon’s heating inside the assembly, preventing its oxidation. Fig. 3 illustrates the typical welding scheme. The weld was visually examined for surface cracks and gas holes.

The welded assembly was hot-rolled at 650 °C in two stages. Fenn rolling mill (model 103) with 254 mm diameter X 305 mm wide rolls was used. The rolls were adjusted to give a uniform gap to ensure parallelism. In the first stage, the assembly was hot-rolled in 24 passes with an average reduction per pass of 7% up to a thickness of 1.93 mm. Then, the plate became too long to fit into the heating furnace and was air-cooled to room temperature. The excess material from the plate on its front and back was cut at a distance of 50 mm from the uranium foil to reduce the plate’s size. The cut ends were again sealed by TIG welding. After 20 min reheat, the plate was hot-rolled in the second stage of hot-rolling. The plate was rolled in 30 passes to reach the final thickness of 0.59 mm, with an average percent reduction of around 3.5%. The total hot-rolling reduction was 95%, performed in 54 rolling passes. Before the first pass, the assembly was heated for 30 min. Between passes, the assembly was reheated for 10 min. After the last pass, the plate was annealed for 30 min at 650 °C. Fig. 4 shows the assembly going into the rolls (A) and coming out of the rolls (B).

A rotation scheme was adopted after each hot-rolling pass. The aim was to distribute the end defects (thickening of the uranium foil at its ends) to maximize the homogeneity in the uranium foil’s thickness at the end of the hot-rolling. The rotation scheme also prevents cambering. Fig. 5 illustrates the rotation scheme adopted in hot rolling.

The plate got from hot-rolling was radiographed to locate the uranium foil. The bonded material was cut off all four sides of the plate. After, the plate was opened to remove the uranium metal

Table 1
Density and impurities of uranium metal.

Uranium Total (%)	98.8 ± 0.5				
Density (g/cm^3)	18.7				
Element	(µg/g)	Element	(µg/g)	Element	(µg/g)
Li	<0.1	Co	4.7 ± 0.3	Eu	<0.1
B	<0.4	Ni	12.2 ± 0.5	Gd	<0.1
Mg	3.8 ± 0.2	Cu	<0.5	Dy	<0.2
Si	<3.0	Zn	<0.1	Ti	0.96 ± 0.05
Ca	2.9 ± 0.3	Mo	<3.0	Ta	<0.1
V	1.6 ± 0.8	Cd	<0.1	W	<0.4
Cr	17.6 ± 0.5	Ba	<0.2	O	1115
Mn	15.6 ± 0.1	Pb	<6.0	C	600
Fe	89 ± 4	Sn	107 ± 30	S	70
Al	55 ± 1	Sm	<0.4	H	27

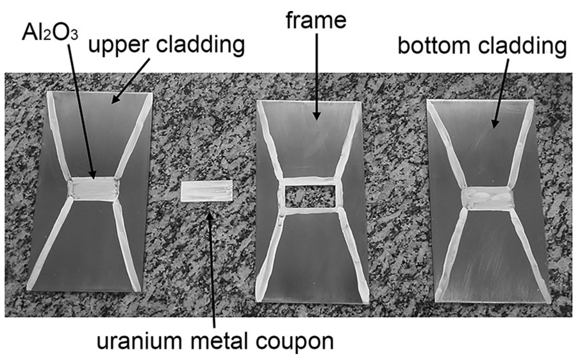

Fig. 2. Picture-frame components of assembly for hot-rolling.

Fig. 3. Welded assembly ready for hot-rolling.

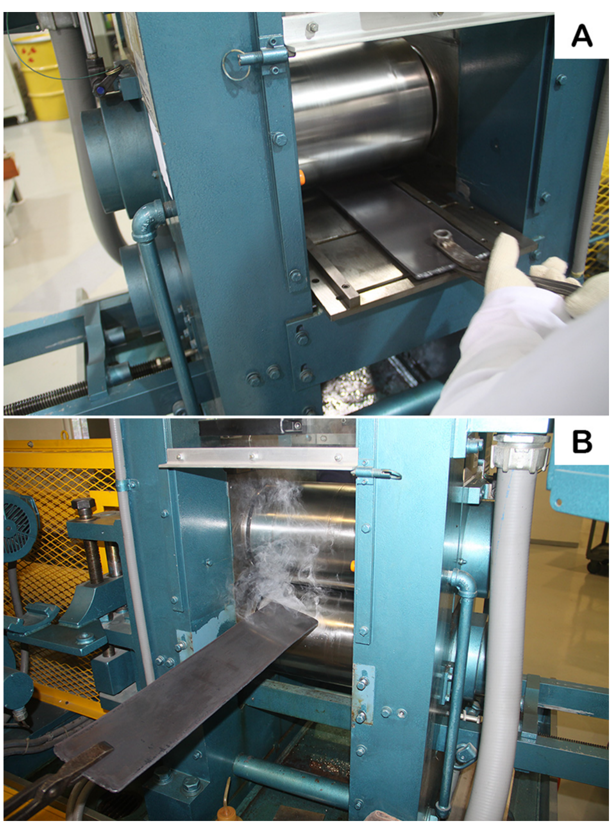

Fig. 4. Illustration of hot-rolling. (A) assembly going into the rolls. (B) assembly coming out of the rolls.

foil, as shown in Fig. 6. Three uranium foils were fabricated. Thickness was measured in 18 positions according to the scheme presented in Fig. 7. The width was measured in 3 positions, and length was measured in one position, as shown. The resulting foil thickness was 250–300 µm. The foil was about 340 mm in length and 65 mm wide.

The uranium foil was etched in a 50% nitric acid / 50% water solution to remove oxide (5 min). After etching, the foil was washed with water, followed by ethyl alcohol washing. Then, the foil was radiographed to inspect for defects. Based on the radiographic image, lines were drawn that guided the cut of 4 to 5 individual pieces (depending on the extension of the end defects). A radiographic scanner was used to get the image and mark the position where the samples were cut. Fig. 8 illustrates the typical radiographic image of uranium foil and the lines drawn to orientate cutting the individual foils for cold-rolling (small cambering can be noted). The foil was then cut into rectangular pieces suitable for cold rolling (60 X 50 mm).

2.3. Cold-rolling of uranium foils

The foils were cold-rolled to accurately achieve the specified thickness of 125 ± 13 µm, according to the ANL specification published by Vandegrift et al. (2016) in Appendix A-1 (page A-231). The uranium foils were cold-rolled directly between polished hardened steel rolls of a goldsmith rolling mill with 60 mm diameter X 120 mm wide rolls. The pass schedule varied depending on the initial hot-rolled foil thickness. In general, 17 cold-rolling passes were required for 55% total reduction, with an average reduction per pass of 5%. After cold-rolling, the thin uranium foils were radiographed to inspect for internal defects and cut to the dimensions 44 ± 2 mm width and 76 ± 2 mm length according to ANL specification published by Vandegrift et al. (2016) in Appendix A-3 (page A-270). A total of 14 thin foils were manufactured. The typical mass of the thin uranium foil was 7.9 g. The foils were measured for thickness in 9 positions (see Fig. 9) using a 0.001 mm precision digital micrometer (see Fig. 10). Length and width were measured in four positions using a 0.01 mm precision caliper. The foil's geometry is customizable for the irradiation geometry, although most foils are 125 µm in thickness (because of heat transfer considerations). The foils were then stored under an inert atmosphere to minimize oxidation before heat treatment and assembly into targets.

2.4. Heat treatment of thin uranium foils

Vandegrift et al. (2016) state that the uranium grains of the foil must be small and randomly oriented to ensure good behavior under irradiation. Cold deformation of uranium metal tends to produce a preferential grain orientation. For this reason, it is necessary to perform a heat-treatment to break the preferred grain orientation and produce a fine grain structure. Conner et al. (1998) developed a method for heat-treating the uranium foil to produce a random small grain structure where the piece needs to be heated into the ß region (T > 668 °C) and then rapidly cooled.

In the present work, the cold-rolled foils were heat-treated at 720 °C for 20 min using a retort that was kept under an inert argon atmosphere and was inserted into a tubular furnace. The retort was argon purged three times before starting heating. Two cooling procedures were used: (1) the retort was slid out of the furnace and was cooled with the help of a fan to <300 °C in 5 min; (2) the uranium foil was sealed inside an envelope manufactured with thin stainless-steel foil (250 µm) and water quenched. The foil microstructure was examined via optical microscopy with polarized light and via XRD (X-ray diffraction). The XRD used a Bruker diffractometer, operating with Cu-Ka radiation at 40 kV and 30 mA, with a scan of 0.02° and 8-second counts per step.

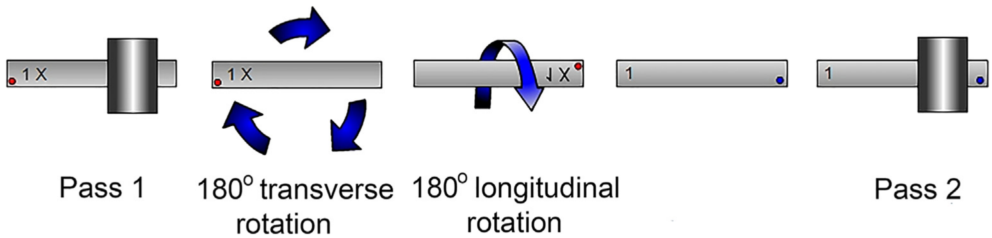

Fig. 5. Rotation scheme of the assembly in hot-rolling.

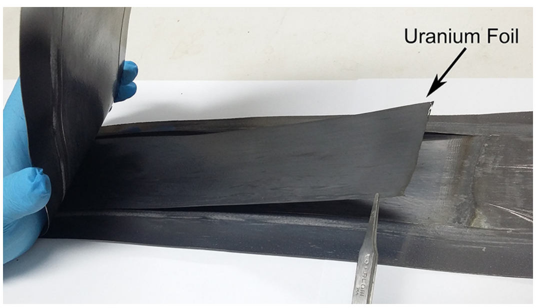

Fig. 6. Opening of the hot-rolled plate to remove the uranium foil.

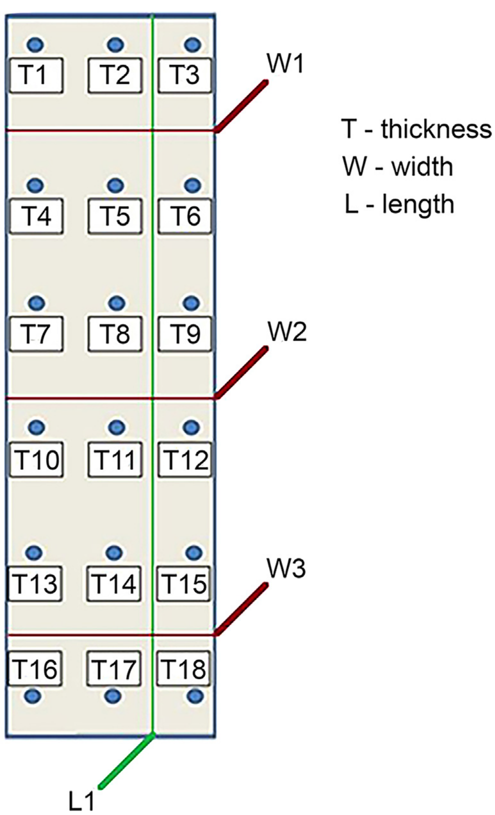

Fig. 7. Hot-rolled thin foils dimensional inspection scheme.

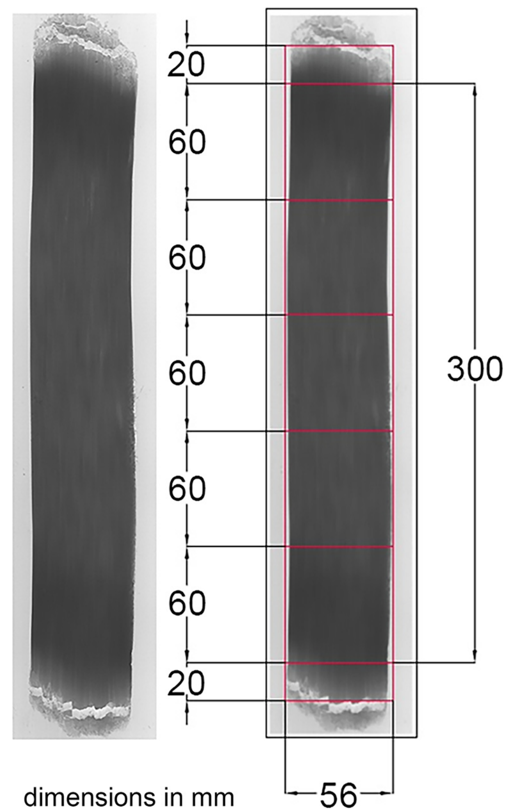

Fig. 8. Typical radiographic image of uranium foil (hot-rolled) and procedure for cutting individual foils for cold-rolling.

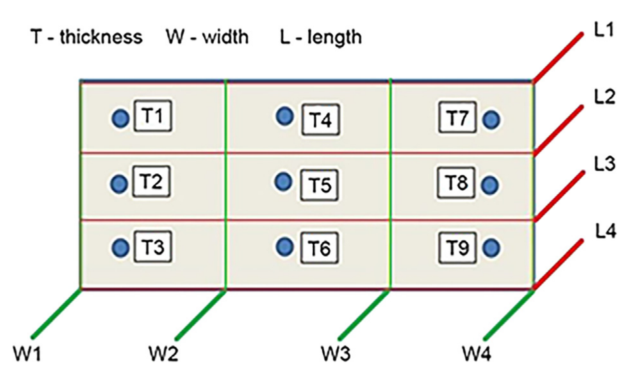

Fig. 9. Cold-rolled thin foils dimensional inspection scheme.

2.5. Thin foil wrapping by the diffusion barrier

Fission recoil barriers (or diffusion barriers) are essential for the high-density annular uranium metal target. Hofman et al. (1996) performed irradiation tests that showed uranium foil bonding to both inner and outer tubes. After irradiation, the inner tube could not be extracted to take out the irradiated uranium foil. A thin foil of diffusion barrier was placed between the uranium foil and the target cladding tubes to prevent the uranium from bonding with the cladding material. This diffusion barrier foil must be thick enough so that the fission fragments do not pass through, preventing bonding. As the foil used as a diffusion barrier must be dis-

Fig. 10. Illustration of foil thickness measuring procedure.

solved together with the uranium sheet, only a few materials could be used, such as nickel, copper, iron, and zinc. A 14 μm thick nickel foil has been used.

The nickel foil was cut so that it entirely wrapped the uranium foil surfaces once folded, as illustrated in the sequence shown in Fig. 11. Additional two millimeters were left at the side and front ends of the nickel foil folded over the uranium foil, forming an envelope. A clean plastic ruler was used to smooth out the nickel foils on all sides, especially in the fold areas.

2.6. Annular target assembling

The heat-treated uranium/nickel foil (uranium foil wrapped with nickel foil) was assembled between two concentric aluminum (6061 T6) tubes, which are the cladding for the uranium foil. The cladding inner and outer tubes were machined to the specified diameters.

An undercut (relief) was machined into the inner tube to hold the uranium foil in position during target assembly. The undercut depth depends on the thickness of the uranium foil added to the nickel foil's thickness (considering the thickness in the folds). According to the target design provided by Wiencek et al. (2009) (Appendix A), the recommended depth is 0.013 ± 0.007 mm less than the total thickness of the wrapped uranium foil. The inner and outer diameters of the inner tube were 26.26 ± 0.05 mm and 28.20 ± 0.05 mm. The inner and outer diameters of the outer tube were 28.35 ± 0.05 mm and 29.98 ± 0.05 mm. These tube dimensions and tolerances allowed the tubes to slide easily past each other while keeping the wrapped uranium foil positioned adequately. The length of the aluminum tubes was 175 mm. After the final assembly of the target, this left-over metal was cut later to prepare for sealing by TIG welding.

A longitudinal line was scribed on the external tube's external surface, which is used as a guide for disassembling the target after irradiation. In the region of this line is a free space for cutting when dismantling the target, as shown in Fig. 12.

The uranium/nickel foil is appropriately wrapped around the inner tube, centralized in the relief region. Then, the inner tube is slid into the outer tube. Alcohol was used as a lubricant. Care was taken to ensure that the nickel foil (fission-recoil barrier) does not get torn. A new procedure (and a new device) was developed and used in the present work to avoid tearing the nickel foil and facilitate the target assembly operation, as discussed in the next session. Care also was taken to ensure that gap between the ends of the uranium foil is lined up with the scribed mark on the outer tube (see Fig. 12). The target was now ready for consolidation and end sealing. After assembling, the targets were radiographed to inspect for uranium/nickel foil positioning. Five targets were assembled.

2.7. Target consolidation

The gaps between the tube and uranium/nickel foil necessary to allow assembly need to be removed through a target consolidation process. Interfaces between the foil and the tubes need to be managed to ensure that the uranium foil temperature does not exceed reactor safety limits. The thermal contact resistance needs to be sufficiently low to ensure good heat transfer from the heat-generating uranium foil through the target's cladding material.

The process for consolidation used by ANL produces a target in which the uranium/nickel foil was held tightly between the two aluminum cladding tubes. As the outer tube is elastically deformed, the ends of the target are removed, and the longitudinal cut is made, the outer tube separates because it is still elastic and quickly releases the uranium foil.

The basic procedures recommended by ANL for target consolidation were adopted in the present work, according to the Vandegrift et al. (2016) report. After the inner tube with the adequately positioned uranium/nickel foil slid into the outer tube, the target was consolidated by plastic deformation of the inner tube using a draw plug. The draw plug was pulled through the inner cladding tube, deforming it as it went. The inner tube in direct contact with the draw plug has been permanently deformed (plastically). The outer tube (not in contact with the draw plug) has been elastically deformed. The draw die prevents plastic deformation of the outer tube. When the expanding force is removed, the outer tube's elastic deformation allows good contact with the inner tube and uranium/nickel foil. The draw die assembly used in the present work is shown in Fig. 13. Fig. 14 shows the draw die assembly device and the target consolidation sequence.

According to Hoyer (2013), residual gaps ("air gap") always occur in this type of assembly, which increases the thermal contact resistance and, therefore, the temperature of the uranium foil. This situation poses a problem for the target's performance under irradiation, as the reactor's technical specifications include a limit on the maximum temperature for the target. Hoyer (2013) studied the air gaps after consolidation and verified that air gaps are visible on the foil area's cross-section if the deformation is too small during target consolidation. Too large of an air gap will prevent good thermal contact, but minimal gaps are necessary for fission gas expansion. Thus, according to Hoyer (2013), few air gaps are necessary, just not large air gaps. Based on the amount of heat generated, the allowable gap space is proportional.

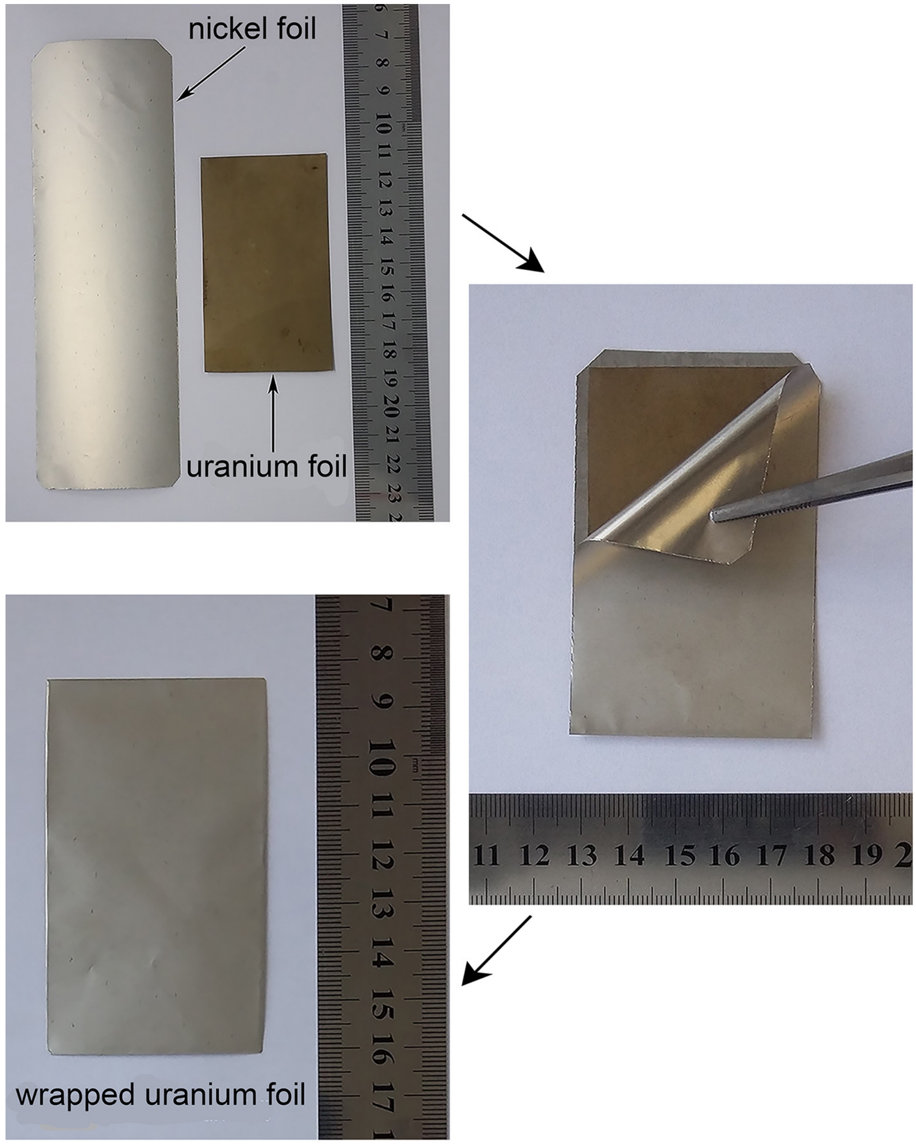

Fig. 11. Sequence for wrapping uranium foil with nickel diffusion barrier foil.

No recommendation was found in the literature for the maximum acceptable size for air gaps. The air gaps depend on the draw plug's diameter, which was calculated according to the target dimensions. According to the ANL procedure, the size of the draw plug required for target consolidation was calculated by subtracting the outer diameter (OD) of the inner tube from the inner diameter (ID) of the outer tube, and finally adding 0.01 mm (see the eq. 1 below) (Vandegrift et al., 2016). Two plug sizes were used in the present work, as discussed in the next section. Fig. 15 illustrates the draw plug.

Plug diameter = ID outer tube – OD inner tube + 0.01 mm (1)

Lubrication was done by coating the draw plug and the interior of the target with graphite Neolube® (colloidal graphite in the isopropanol). Plugs were cleaned after each use to avoid an accumulation of 6061-T6 aluminum material. Fig. 16 shows a consolidated target.

Targets were radiographed to inspect for uranium/nickel foil positioning. Samples were destroyed for viewing cross-sections until the optical microscope. The samples were sanded and polished. Several size sand grits were used, ranging from 350 grit size to 1200 grit size for polishing. Aluminum oxide was used in the polishing stage.

2.8. End sealing

The assembled targets were cut by machining to their final length (153 mm). Chamfers were cut (0.5 mm X 45°) on the inner and outer surfaces after facing. Copper chills have been installed around and inner the target to restrict heating. The target was rotated at 5 rpm, and a DC 10 A welding current was used. A 3 mm diameter thoriated-tungsten electrode was used, and the electrode/target distance was maintained between 3 mm and 5 mm. Fig. 17 shows the welding operation.

3. Results and discussion

3.1. Hot-rolling of coupons

Three coupons were take-off from the primary ingot to analyze the reproducibility of the hot-rolling procedure, which showed to

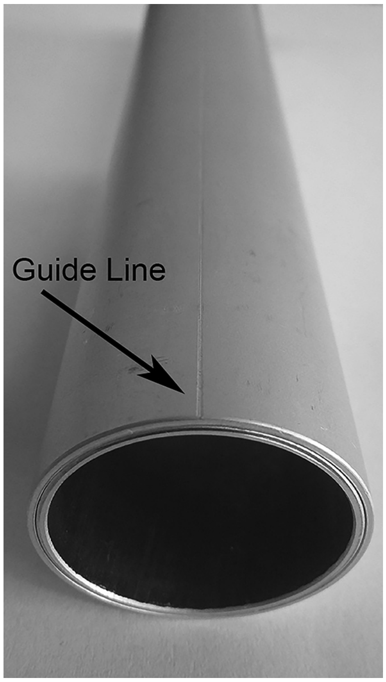

Fig. 12. Guideline for target dismantling after irradiation.

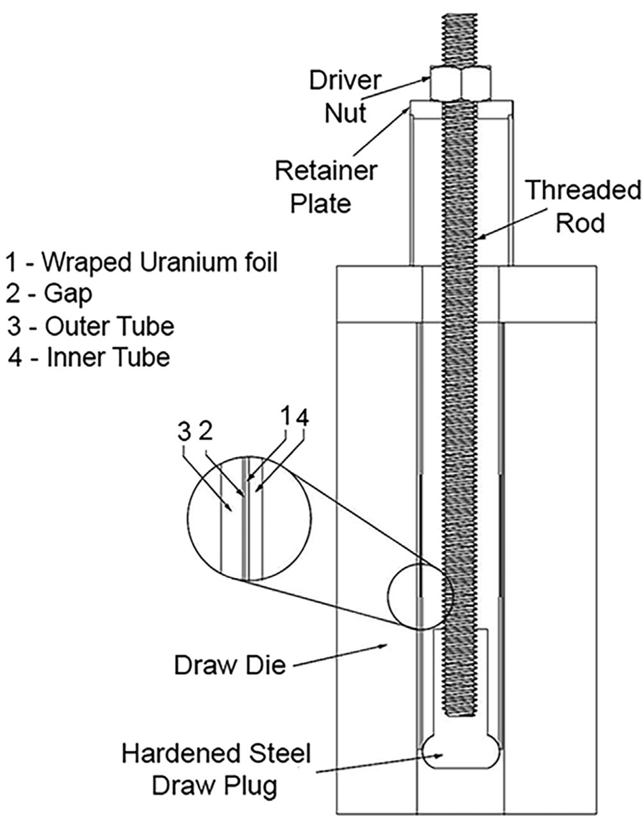

Fig. 13. Sketch of draw die assembly.

be quite reproducible. The dimensions of the three hot-rolled uranium foils are presented in Table 2. Thickness was measured in 18 positions according to the scheme presented in Fig. 7.

In the first hot-rolling attempt, the protective oxide layer to prevent bonding was applied over the entire internal surface of the cladding plates, leaving 20 mm uncovered at the edges, as recommended by Vandegrift et al. (2016). As the assembly was wholly closed by welding, the gases remained trapped inside the assembly. After a certain point in the rolling process, the sheet became thinner, and a giant bubble formed, preventing the steel components from forming bonds. The bubble caused the welds in the longitudinal edges to break. As a result, the plate wrinkled, and creases were created, as shown in Fig. 18.

This problem caused irreparable defects in the uranium foil. For this reason, the procedure for applying the anti-bonding layer was changed, adopting the scheme illustrated in Fig. 2. This new system allowed the gases to escape by "paths" to the ends of the assembly when the welds were broken because of high pressure, allowing the assembly's components to bond outside the protected regions. The breakage of the weld was perceived by the snap that could be heard. When the break occurred, the opened extremities were welded again. This procedure gave the plate greater rigidity when its thickness became small, avoiding the problem illustrated in Fig. 18. After this correction, three plates were hot-rolled successfully. The radiographic inspection did not show any visible defects.

According to the Vandegrift et al. (2016) report, ANL uses yttrium-oxide/alcohol slurry as protection to prevent bonding. Other more available and inexpensive options were tested in the present work (aluminum oxide, titanium oxide, and organic compounds). Aluminum oxide (<3 μm) showed to prevent bonding efficiently. So, aluminum-oxide/alcohol slurry having a consistency of a thin paste was selected to be used.

3.2. Cold-rolling of uranium foils

Cold-rolling had been reproductive and controllable. In the first operations, two foils were reproved for thickness lower than the minimum specified (112 μm). However, the rolling procedure was controlled properly after the two first cold-rolling operations, and no more rejections occurred. Radiography showed good homogeneity with no detectable defects (see Fig. 19), and the optical micrography presented in Fig. 20 shows uniform thickness. Table 3 presents the dimensions of twelve uranium foils resulting from cold-rolling. Thickness was measured in 9 positions according to the scheme presented in Fig. 9.

3.3. Heat-treatment of thin uranium foils

According to Wiencek et al. (2009), a textured preferential grain-orientation with the plane (1 0 0) parallel to the rolling plane is observed in the rolling of uranium metal. Highly textured uranium exhibits severe anisotropic growth when irradiated. This growth can cause the uranium foil to bond to the cladding tube, preventing the foil from being removed after irradiation. Anisotropic growth could even cause the target's cladding to fail during irradiation. So, it is necessary for a heat treatment to produce a fine-grained, randomly oriented structure to avoid this problem.

Conner et al. (1998) proposed a method to analyze preferred orientation based on inspection of the ratio of the hkl reflections 111 and 113. The authors used the value of the ratio 111/113 equals 6 as a reference for unoriented uranium. This reference value showed to vary significantly from 6 in cold-rolled and not heat-treated samples. One or two heat-treatment cycles must be done to prevent preferred orientation. For 50 to 60% cold-rolling, one cycle is enough. For 30 to 40% cold-rolling, two cycles are necessary. The number of heat-treatment cycles depends on the amount of strain in the piece once the uranium needs to recrystallize to remove the preferred orientation (Conner et al., 1998).

Table 4 presents the results for the ratio 111/113 of the hkl reflections calculated for the heat-treatments used in the present work (quenching and air cooling). This result indicates that cooling

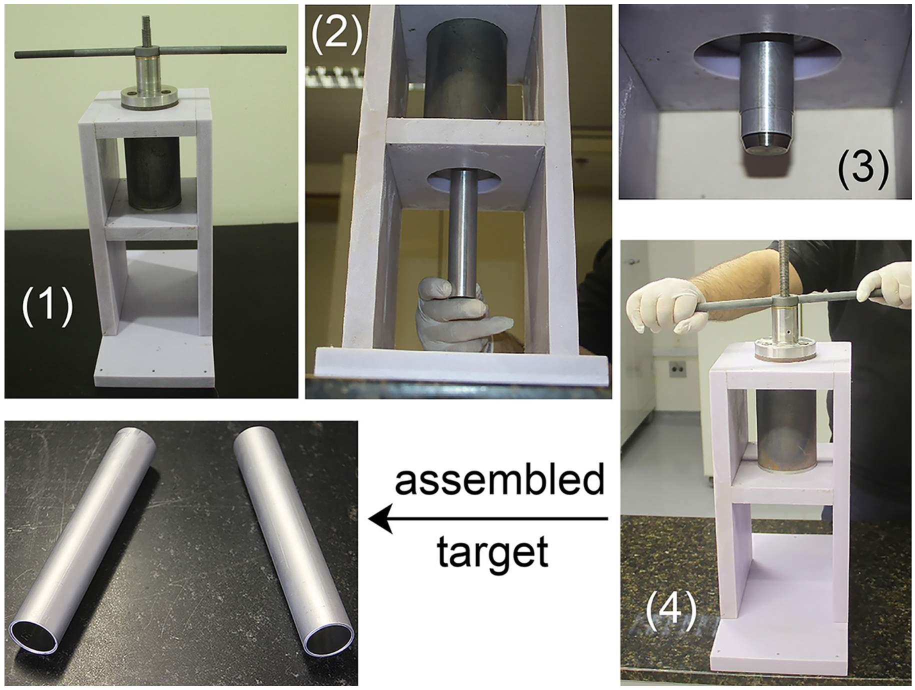

Fig. 14. Illustration of target consolidation sequence.

Fig. 15. Illustration of draw plug (size 26.40 mm).

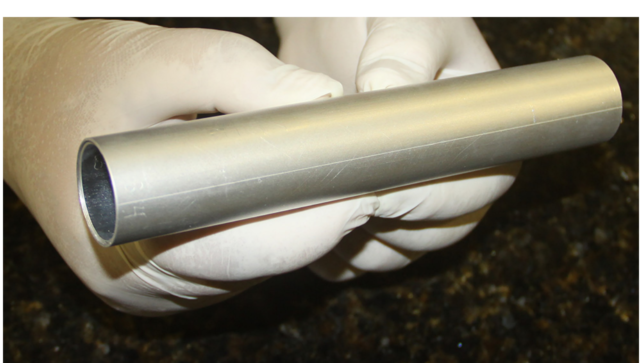

Fig. 16. Illustration of a consolidated target.

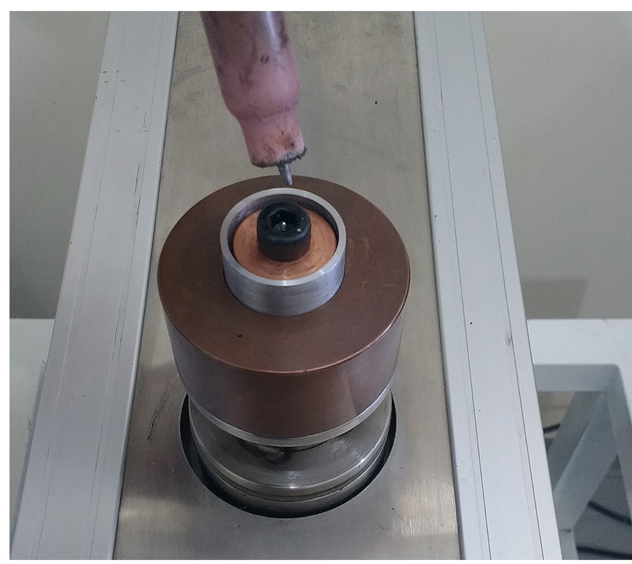

Fig. 17. Welding for end sealing of target.

at an 85 °C/min rate is enough to eliminate the preferred orientation. For 50% cold rolling, Conner et al. (1998) got a value of 6.25 ± 15%, which is near the value got in the present work for 55% cold rolling.

The resulting microstructure (see Fig. 21) showed equiaxial very small grains. The maximum grain size was decreased from 80 μm for the cold-rolled foil to 42 μm for the heat-treated foil (cooled 5 min to 300 °C). The mean grain size decreased from 20 μm to 11 μm. The grain size was measured through image analysis. The aspect ratio (ratio between the largest and smallest grain size) measured for the grain structure of the cold-rolled foils showed a tendency for grains to elongate according to a preferen-

Table 2
Dimensions of uranium foil after hot-rolling (mm).

	Hot-rolled foil 1			Hot-rolled foil 2			Hot-rolled foil 3		
	T	W	L	T	W	L	T	W	L
1	0.285	67	338	0.287	69	355	0.300	66	320
2	0.298	67		0.287	69		0.299	65	
3	0.298	66		0.290	68		0.302	65	
4	0.255			0.265			0.284		
5	0.260			0.257			0.276		
6	0.254			0.255			0.280		
7	0.250			0.251			0.266		
8	0.251			0.253			0.263		
9	0.260			0.258			0.262		
10	0.260			0.259			0.260		
11	0.258			0.258			0.262		
12	0.259			0.258			0.262		
13	0.260			0.262			0.275		
14	0.258			0.260			0.281		
15	0.252			0.260			0.278		
16	0.269			0.279			0.289		
17	0.287			0.282			0.294		
18	0.290			0.287			0.295		

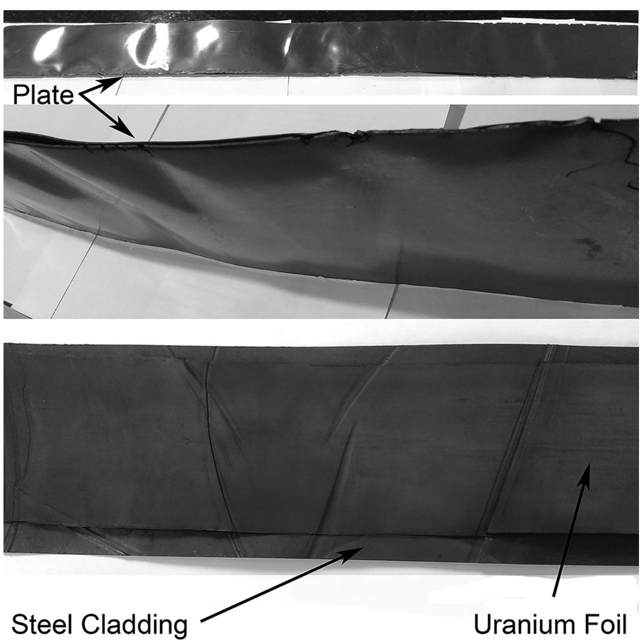

Fig. 18. Defects in the hot-rolled plate, which were transferred to the uranium foil.

tial direction. This tendency was not observed for heat-treated foil (cooled 5 min to 300 °C). It can be noted that the grain sizes resulting from the present work are almost 6 times lower than the grain size presented by Conner et al. (1998) (by visual comparison) for comparable cold-rolling deformation (55% at this work and 60% for Conner et al., 1998). This observation shows that the cooling rate after the heating period is not the most critical variable. The reason for this quite different result is still unclear.

3.4. Target assembling

Aluminum 6061 T6 tubes were selected to have a composition of diameters that allowed comfortable assembling. The difference between the outer tube's inner diameter ($\varnothing_i$ OT) and the inner tube's outer diameter ($\varnothing_o$ IT) was kept in the 0.1–0.2 mm range. Uranium thin foils were selected, and the undercuts were machined in the inner tubes with the base on the thickness of the wrapped foils. The undercut depth was defined to accommodate the uranium/nickel foil (uranium foil wrapped with nickel foil), keeping it 0.013 ± 0.007 mm above the inner tube's surface level, according to the ANL specification. Table 5 presents the characteristics of the targets that were assembled. The minimum assembly clearance (distance between the wrapped uranium foil and aluminum outer tube) was kept at a 0.05 mm minimum.

Targets were assembled manually. The uranium/nickel foil was wrapped around the inner tube in the relief that was machined. For assembling, the procedure reported by Vandegrift et al. (2016) was adopted. The foil was pressed onto the inner tube's surface using fingers, and the inner tube was pushed into the outer tube. Great care was taken to ensure that the nickel foil did not get torn, which was very difficult. Many of them were torn during the assembly, and all the work had to be redone. During insertion, the nickel foil crinkles and often torn, as shown in Fig. 22.

An innovative method for target assembling has been developed to facilitate the assembly operation. The uranium/nickel foil was pre-conformed into a tubular shape to wrap by itself the inner tube, without operator intervention, as shown in Fig. 23. No further action by the operator's fingers was necessary. The pre-conformation was made with the aid of a specially designed device built to do this task, shown in Fig. 24. The assembling operation using the new procedure resulted in a secure and easy operation, as illustrated in Fig. 25.

After the tubes have slid past one another with the uranium/nickel foil adequately positioned, the location of the gap between the ends of the foil was marked on the outer tube for future disassembly reference. A longitudinal line was scribed to guide the cut for dismantling the target after irradiation. Radiographic inspection certified that the uranium/nickel foil was positioned correctly, as shown in Fig. 26.

3.5. Target consolidation

Draw plug size was calculated according to equation 1, as recommended by Vandegrift et al. (2016). Table 6 presents the calculations for each assembled target according to the data presented in Table 5. Draw plugs were fabricated with 26.41 mm and 26.49 mm diameters.

Target 1 was consolidated using a 26.49 mm diameter draw plug, and target 2 was consolidated with a 26.41 mm diameter draw plug. After consolidation, both targets showed continuous air gaps about 20 μm thick in the interface nickel/aluminum all around the target perimeter, as illustrated in Fig. 27. A continuous

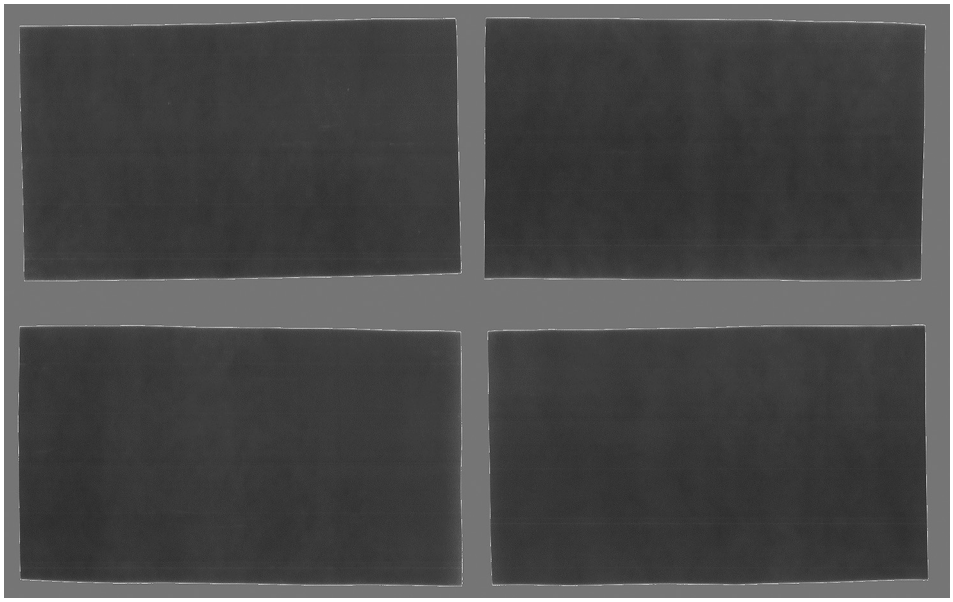

Fig. 19. Radiographies of four cold-rolled uranium foils.

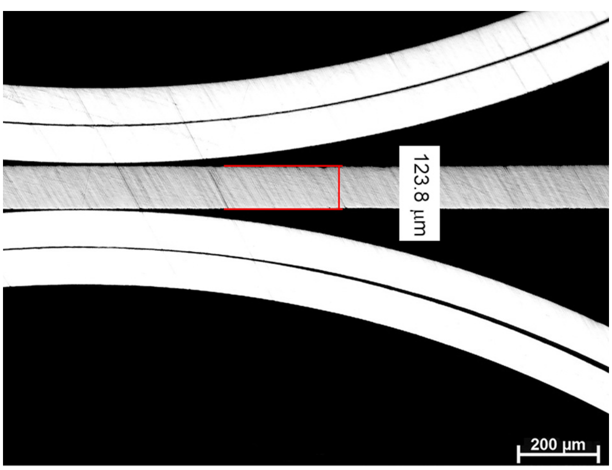

Fig. 20. Transversal section of a cold-rolled uranium foil (foil 11-D).

around 6 µm gap was also observed in the interface uranium/nickel.

No specification (or even recommendation) was found in the literature for the maximum air gap value. Values between 10 and 30 µm are established as acceptable by Olivares et al., 2015. Hoyer (2013) stated that no sample was perfectly without air gaps and considered acceptable isolated gaps with about 30 µm in thickness and around 1 mm in length. For this reason, a continuous air gap, even if small, was considered not acceptable in the present study. The problem was attributed to the minimal effective deformation applied to both targets. Only 17 µm deformation was applied when disregarding all clearances and considering the portion of uranium/nickel foil above the relief. For this reason, it was decided to increase the deformation as much as possible by applying the largest available size plug to the target with the smallest internal diameter. Therefore, target 5 was assembled by using the 26.49 mm size plug. This operation provided an actual deformation of 0.158 mm. The result is shown in Fig. 28. Although much smaller (6 µm), a continuous air gap could still be seen.

Table 3
Dimensions of cold-rolled uranium foils (according to Vandegrift et al.(2016), ANL specification is 112 µm–137 µm).

Foil	Thickness (µm)									Width (mm)				Length (mm)			
	1	2	3	4	5	6	7	8	9	1	2	3	4	1	2	3	4
*8-A	100	106	100	102	105	103	98	104	101	42.01	42.07	42.03	42.05	77.80	77.50	77.30	77.32
*8-B	110	112	112	119	116	106	114	114	113	43.94	44.25	44.25	43.85	76.56	76.72	76.62	76.61
8-C	123	131	123	128	133	121	117	126	124	43.90	44.14	43.97	44.01	75.86	76.25	76.45	76.86
8-D	134	134	134	126	130	128	120	123	119	44.36	44.39	44.12	43.97	76.21	76.43	76.49	76.20
8-E	132	134	134	135	134	134	129	130	134	43.67	44.31	44.23	44.24	76.16	76.06	76.15	76.01
10-A	124	131	124	128	138	133	132	137	133	44.94	44.80	44.61	44.25	75.78	75.82	76.21	76.28
10-B	122	127	123	125	132	128	122	130	124	43.14	43.22	42.71	43.90	76.14	75.93	75.86	75.74
10-C	121	133	119	126	131	120	117	117	113	43.71	43.69	44.00	44.43	75.19	75.08	75.06	74.99
10-D	128	130	127	134	131	127	135	132	128	43.91	43.95	44.28	44.00	75.61	75.78	75.64	75.63
10-E	118	124	120	127	127	124	115	120	114	44.87	44.89	44.78	44.33	76.26	76.54	76.80	76.57
11-A	124	130	122	122	123	116	120	124	122	42.77	42.93	42.59	42.04	74.98	75.54	75.61	75.29
11-B	128	126	121	126	122	122	118	118	118	43.96	44.02	44.23	44.01	75.80	75.71	75.66	75.75
11-C	133	136	135	127	126	128	115	118	118	44.69	44.95	44.88	44.87	76.48	76.32	75.94	75.37
11-D	126	127	125	122	123	124	121	124	126	44.16	44.19	44.12	44.20	75.89	75.95	75.95	75.19

* rejected due to low thickness.

Table 4
111/113 ratio of the hkl reflections measured in XRD diffractograms.

Cooling Rate	111/113 ratio
Cold-rolled (as fabricated)	0.5
Quenching (fist cycle)	5.0
Quenching (second cycle)	6.1
Air cooled (5 min to 300 °C))	6.5
Furnace cooled (20 min to 300 °C) (retort is kept inside furnace)	1.9

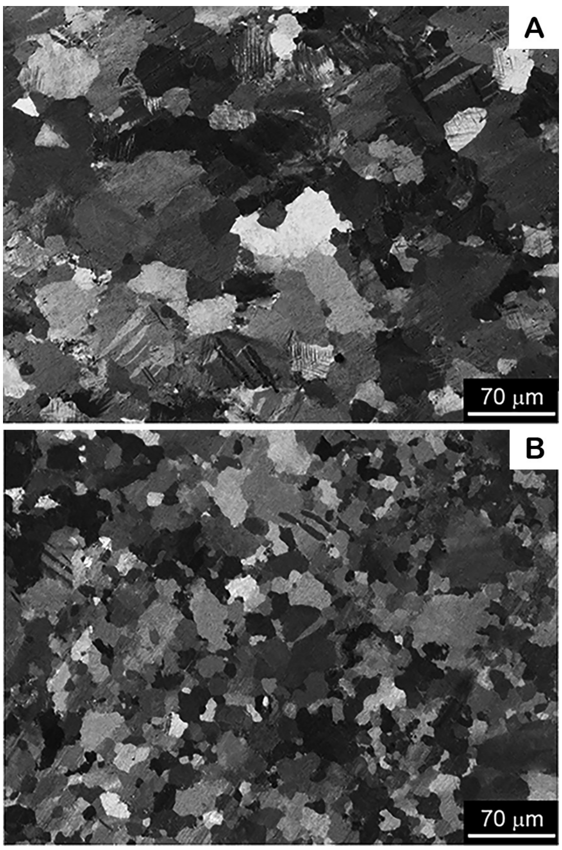

Fig. 21. Grain structure of cold-rolled foil. (A) not heat-treated. (B) heat-treated (air-cooled).

Hoyer (2013) concluded that the deformation of 0.254 mm was the best condition for the maximum closing of air gaps. Therefore, it was decided to apply this level of deformation to consolidate target 3. For this, a new draw plug was manufactured with a diameter of 26.60 mm, which would provide an actual deformation of 0.258 mm. Unfortunately, this consolidation test failed because the draw plug stuck inside the target.

Fig. 22. Pictures illustrating difficulty to assembly targets by using ANL procedure.

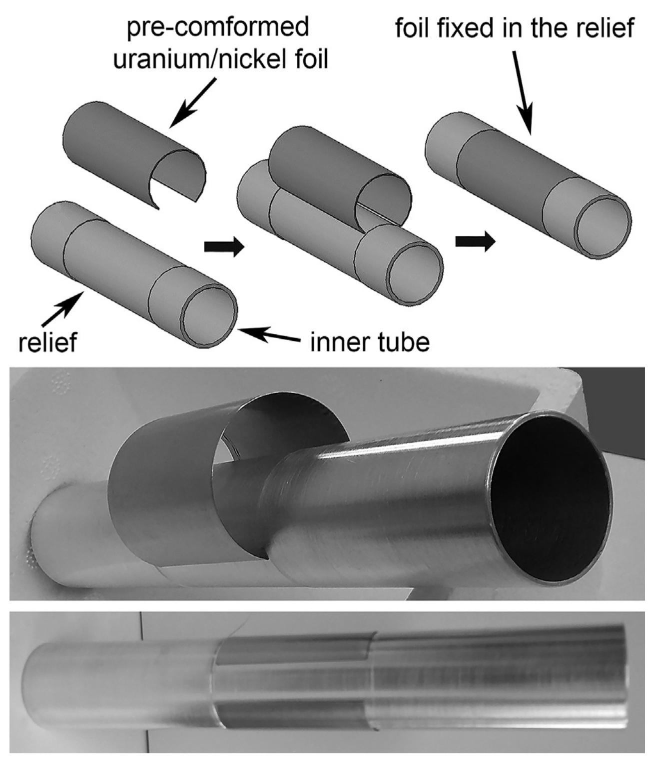

Fig. 23. Innovative procedure for assembling targets.

Table 5
Characteristics of the five targets that were assembled (dimensions in mm).

Target	Inner Tube (IT)		Outer Tube (OT)		$\varnothing_i$ OT – $\varnothing_o$ IT	Wrapped Foil Thickness	Relief Depth	Assembling Clearance
	$\varnothing_o$	$\varnothing_i$	$\varnothing_o$	$\varnothing_i$				
1	28.16	26.30	29.95	28.34	0.18	10D – 0.191	0.184	0.083
2	28.19	26.24	30.02	28.35	0.16	10E – 0.183	0.176	0.073
3	28.23	26.22	30.02	28.36	0.13	11B – 0.184	0.176	0.057
4	28.18	26.24	29.93	28.30	0.12	11C – 0.192	0.182	0.050
5	28.22	26.21	29.96	28.35	0.13	11D – 0.183	0.175	0.057

$\varnothing_o$ = outer diameter and $\varnothing_i$ = inner diameter.

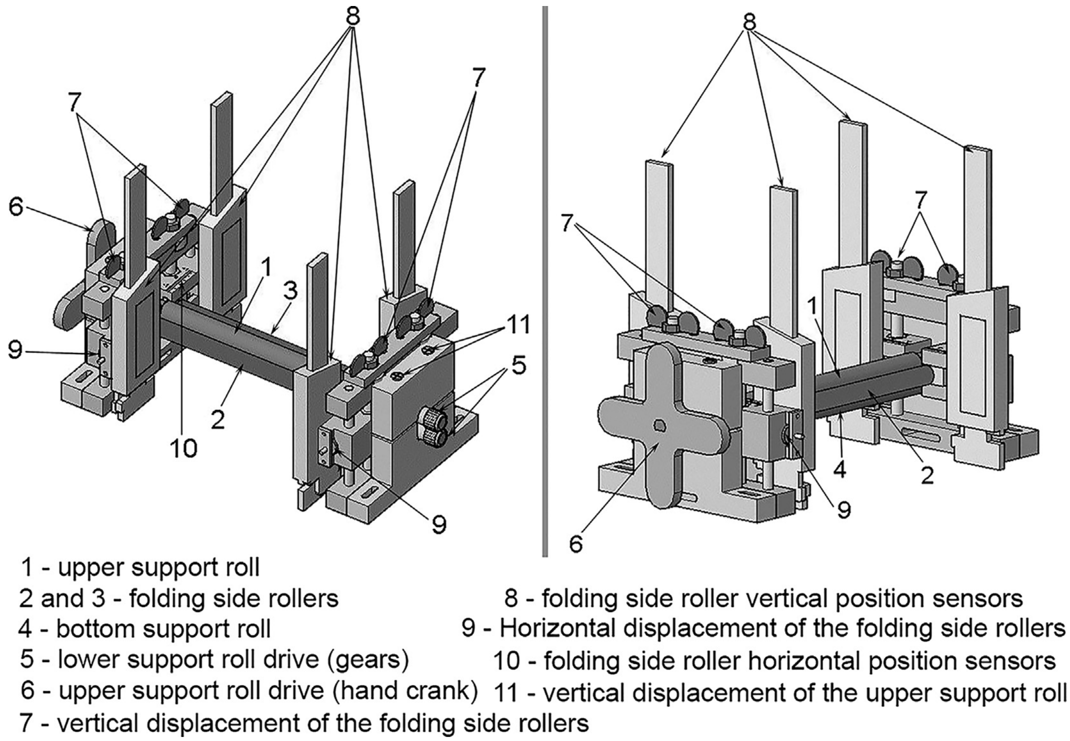

Fig. 24. Device designed for pre-conforming the uranium/nickel foil.

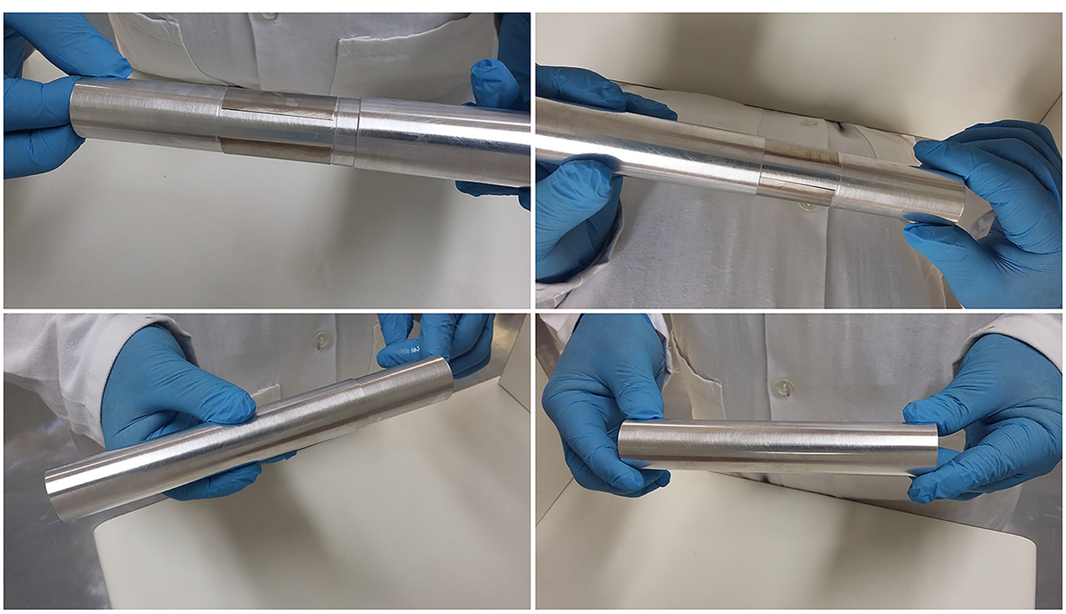

Fig. 25. Target assembly steps with the new procedure (pre-conformed uranium/nickel foil).

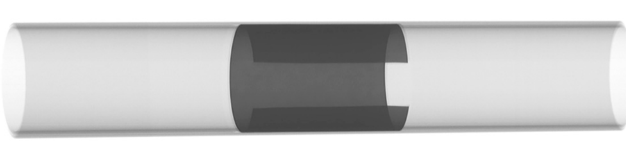

Fig. 26. Typical radiography of an assembled target.

These results showed that the consolidation step proved to be the most problematic among all the steps to manufacture this type of target. Controlling deformation to eliminate air gaps proved to be very difficult. In the present work, the deformation needed would be between 0.158 mm and <0.258 mm, a range too small to be well-controlled. Even so, isolated air gaps should remain. The consolidation method of using the hydro-forming process appears to be advantageous and will be studied in future work. Hydro-forming applies a high-pressure fluid to the inside of the inner tube, which causes its expansion. The primary conceptual difference between the draw plug and the hydro-forming methods

Table 6
Draw plug size calculation (dimensions in mm).

Target	Inner Tube (IT)		Outer Tube (OT)	$\varnothing_i$ OT – $\varnothing_o$ IT	Plus 0.01	Plug Size
	$\varnothing_o$	$\varnothing_i$	$\varnothing_i$			
1	28.16	26.30	28.34	0.18	0.19	26.49
2	28.19	26.24	28.35	0.16	0.17	26.41
3	28.23	26.22	28.36	0.13	0.14	26.36
4	28.18	26.24	28.30	0.12	0.13	26.37
5	28.22	26.21	28.35	0.13	0.14	26.35

$\varnothing_o$ = outer diameter and $\varnothing_i$ = inner diameter.

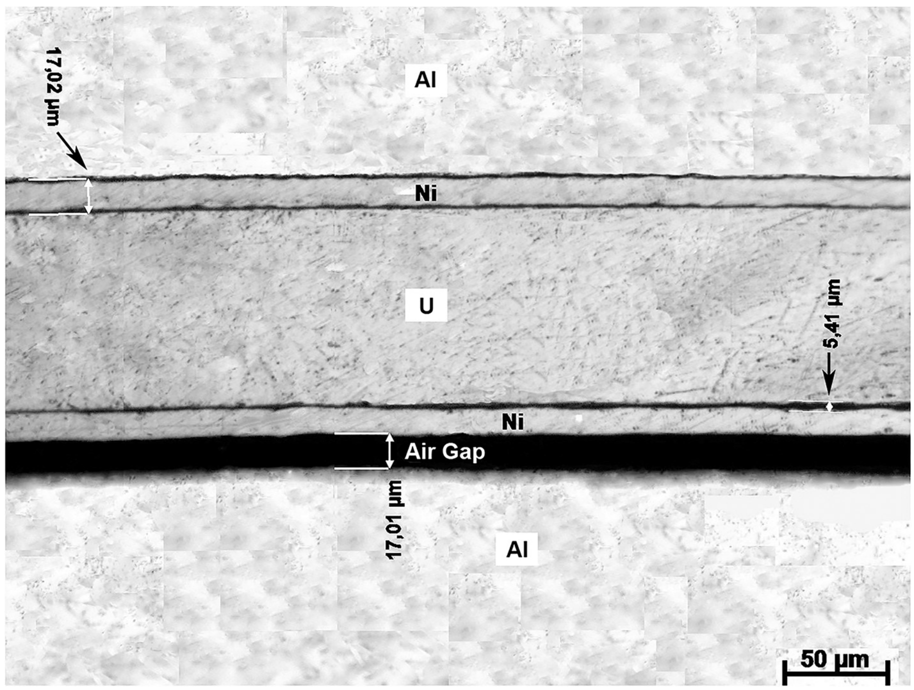

Fig. 27. Optical micrography illustrating a continuous residual air gap in a target assembled according to the recommendation of ANL (target 1, plug size 26.49 mm).

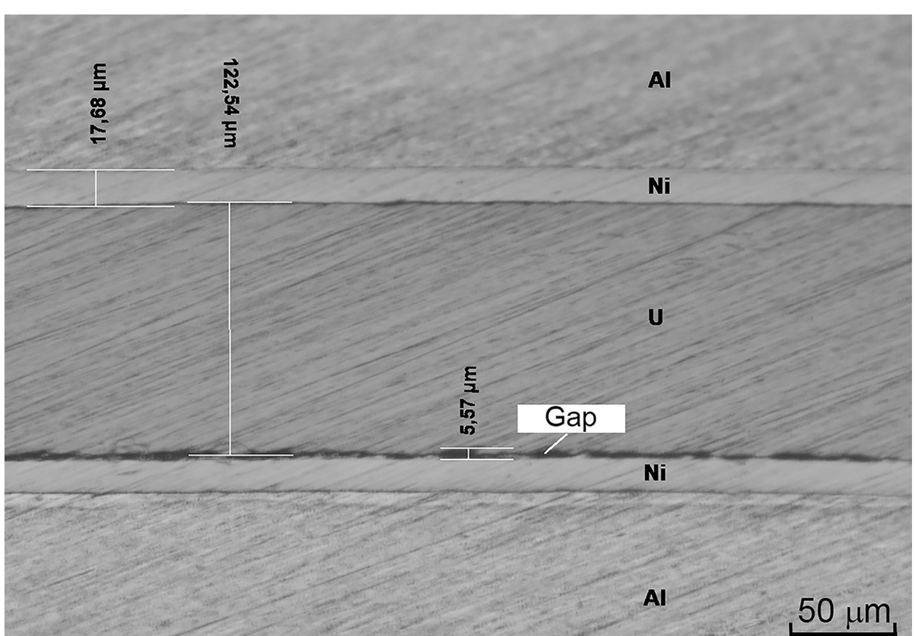

Fig. 28. Optical micrography illustrating a continuous residual air gap in target 5 applying plug size 26.49 mm (deformation of 0.138 mm).

Fig. 29. Illustration of a typical end sealing weld.

Fig. 30. Optical micrography illustrating a typical end sealing weld.

for target consolidation is how the radial force is developed. The hydro-forming method applies radial force directly.

The radiographic inspection carried out after the consolidation step showed that the uranium/nickel foil remained in place after all the tests.

3.6. End sealing

TIG welding to seal the ends of the target proved to be very dependent on the operator's skill. However, after a few attempts, a good quality sealing weld was achieved, as shown in Fig. 29. Fig. 30 shows an optical micrograph of the sealing weld cross-section. TIG welding showed to be acceptable for sealing the targets.

4. Conclusions

A great deal of experience in the manufacture of uranium metal tubular targets was gained with this work. The main manufacturing steps adopted internationally were studied appropriately, defining the main manufacturing parameters. Some manufacturing procedures have been changed in view of the advantages over the procedures adopted internationally. Quenching showed to be unnecessary, as a fine grain structure could be obtained with a cooling rate of about 84 °C/min (cooled 5 min to 300 °C). An innovative method was successfully developed and applied, which facilitated assembling the uranium/nickel foil in the inner tube, reducing the need for rework. The target consolidation step proved to be particularly difficult. Air gaps could not be suppressed entirely. The hydro-forming technique is planned to be studied for the execution of this step. Studies are underway to define the specification of the target for the Brazilian Multipurpose Reactor (RMB).

CRediT authorship contribution statement

Michelangelo Durazzo: Project administration, Conceptualization, Methodology, Supervision, Validation, Funding acquisition, Writing - original draft, Writing - review & editing. **Jose A.B. Souza:** Investigation, Resources, Data curation. **Ricardo F. Ianelli:** Investigation, Methodology, Resources. **Eriki M. Takara:** Investigation, Methodology, Resources. **Jose S. Garcia Neto:** Investigation, Methodology, Resources. **Adonis M. Saliba-Silva:** Writing - review & editing. **Elita F. Urano de Carvalho:** Visualization.

Declaration of Competing Interest

The authors declare that they have no known competing financial interests or personal relationships that could have appeared to influence the work reported in this paper.

Acknowledgments

The authors are grateful to CNPq (National Council for Scientific and Technological Development) for the research grants 454147/2017-1 and 304034/2015-0 provided for this work. The authors would also like to thank São Paulo Research Foundation (FAPESP) for the research grants 2015/08922-0 and 2018/18228-1. The authors also want to give special thanks to Prof. Jaime Ramon Lisboa Lineiros from Chilean Nuclear Energy Commission for the valuable technical contribution provided during his visit to IPEN-CNEN/SP.

References

Ali, K.L., Khan, A.A., Mushtaq, A., Imtiaz, F., Zial, M.A., Gulzar, A., Farooq, M., Hussain, N., Ahmed, N., Pervez, S., Zaidi, J.H., 2013. Development of low enriched uranium target plates by thermo-mechanical processing of UAl_2-Al matrix for production of 99Mo in Pakistan. Nucl. Eng. Des. 255, 77–85. https://doi.org/10.1016/j.nucengdes.2012.10.014.

Barnowski, R., 2011. Insourcing Nuclear Medicine, Journal of Science Policy & Governance 1, 1-4 (available at: https://www.sciencepolicyjournal.org/uploads/5/4/3/4/5434385/_insourcing_nuclear_medicine.pdf.

Briyatmoko, B., Guswardani, B., Purwanta, S., Permana, S., Basiran, D., Kartaman, M., 2007. Indonesia's current status for conversion of Mo-99 production to LEU fission. In: Proceeding of International Meeting on Reduced Enrichment for Research and Test Reactors, Prague, Czech Republic, 23-27 September, 2007 (available at: http://www.rertr.anl.gov/RERTR29/index.html.

Brown, M.A., Jerden Jr., J.L., Gelis, A.V., Stepinski, D.C., Wiedmeyer, S., Youker, A., Hebden, A., Vandegrift, G.F., 2014. Development of frontend processing to allow use of high-density LEU foil targets in current Mo-99 production facilities. In: 2014 Topical Meeting on Molybdenum-99 Technological Development, Washington, D.C. USA, 24-27 June, 2014 (available at: <http://mo99.ne.anl.gov/2014/pdfs/papers/S11P3%20Paper%20Brown.pdf.

Conner, C., Liberatore, M.W., Mutalib, A., Sedlet, J., Walker, D., Vandegrift, G.F., 1998. Progress in developing processes for converting 99Mo production from high to low enriched uranium. Proceeding of International Meeting on Reduced Enrichment for Research and Test Reactors, São Paulo.

Conner, C., Lewandowski, E. F.; Snelgrove, J. L.; Liberatore, M. W.; Walker, D. E.; Wiencek, T. C.; McGann, D. J.; Hofman, G. L.; Vandegrift, G. F.. 1999. Development of annular targets for 99Mo production. Proceedings of the 1999 International Meeting on Reduced Enrichment for Research and Test Reactors (RERTR) held in Budapest, Hungary on October 3-8, 1999. (available at: https://inis.iaea.org/collection/NCLCollectionStore/_Public/35/015/35015949.pdf.

Cols, H.J., Cristini, P.R., Manzini, A.C., 2000. Mo-99 from low-enriched uranium. In: Proceeding of International Meeting on Reduced Enrichment for Research and Test Reactors, Las Vegas, Nevada, 1-6 October, 2000 (available at: http:// www.rertr.anl.gov/Web2000/Title-Name-Abstract/Cristi00.html.

Durazzo, M., Riella, H.G., 2015. Procedures for Manufacturing Nuclear Research Reactor Fuel Elements. OmniScriptum GmbH & Co, KG, Saarbrücken, Germany, p. 2015.

Durazzo, M., Saliba-Silva, A.M., Martins, I.C., Urano de Carvalho, E.F., Riella, H.G., 2017. Manufacturing low enriched uranium metal by magnesiothermic reduction of UF_4. Ann. Nucl. Energy 110, 874–885. https://doi.org/10.1016/j.anucene.2017.07.033.

Hansell, 2008. Nuclear medicine's double hazard: imperiled treatment and the risk of terrorism. Nonprolif. Rev. 15, 185–208. https://doi.org/10.1080/10736700802117270.

Hofman, G.L., Wiencek, T.C., Wood, E.L., Snelgrove, J.L., Suripto, A., Nasution, H., Lufti-Amin, D., Gogo, A., 1996. Irradiation tests of 99Mo isotope production employing uranium metal foils. Proceeding of International Meeting on Reduced Enrichment for Research and Test Reactors.

Hoyer, A., 2013. An investigative approach to explore optimum assembly process design for annular targets carrying LEU foil, Thesis presented to the Faculty of the Graduate School at the University of Missouri, Columbia, December 2013. (available at: https://mospace.umsystem.edu/xmlui/handle/10355/43063.

AEA, 2015. Feasibility of Producing Molybdenum-99 on a Small Scale Using Fission of Low Enriched Uranium or Neutron Activation of Natural Molybdenum, Technical Reports Series no 478, International Atomic Energy Agency. (available at: https://www-pub.iaea.org/MTCD/Publications/PDF/trs478web-32777845.pdf.

IAEA, 2018. Developing Techniques for Small Scale Indigenous Molybdenum 99 Production Using Low Enriched Uranium (LEU) Fission or Neutron Activation. Coordinated Research Project T12018, CRP 193. (Available at: https://www.iaea.org/projects/crp/t12018.

Kaufman, A.R., 1962. Nuclear Reactor Fuel Elements, Metallurgy and Fabrication, Interscience, New York, N.Y, 1962.

Kohut, C., Fuente, M., Echenique, P., Podesta, D., Adelfang, P., 2000. Targets development of low enrichment for production of Mo99 for fission. In: Proceeding of International Meeting on Reduced Enrichment for Research and Test Reactors, Las Vegas, Nevada, 1-6 October, 2000 (available at: I DEVELOP DE WHITE DE LOW ENRIQUECIMIENTO UAL2 FOR PRODUCCIÓN DE 99Mo by FISION (anl.gov).

Mushtaq, A., 2011. Specifications and qualification of uranium/aluminum alloy plate target for the production of fission molybdenum-99. Nucl. Eng. Des. 241, 163–167. https://doi.org/10.1016/j.nucengdes.2010.11.003.

National Academies of Sciences, Engineering, and Medicine, 2016. Molybdenum-99 for Medical Imaging. Washington, DC: The National Academies Press. https://doi.org/10.17226/23563.

Nuclear Energy Agency, 2016. The supply of medical radioisotopes: 2016 medical isotope review: 99Mo/99mTc market demand and production capacity projection 2016-2021. NEA/SEN/HLGMR(2016)2. March 2016. Nuclear Energy Agency (available at: Nuclear Energy Agency (NEA) - The Supply of Medical Radioisotopes: 2016 Medical Isotope Supply Review: 99Mo/99mTc Market Demand and Production Capacity Projection 2016-2021 (oecd-nea.org).

Obadia, I.J., Perrotta, J A., 2010. A sustainability analysis of the Brazilian Multipurpose Reactor Project. In: International Topical Meeting on Research Reactor Fuel Management RRFM 2010, Marrakech, Morocco, 21-25 March, 2010 (available at: https://www.euronuclear.org/download/proceedings-rrfm-2010/?wpdmdl=3046&refresh=5fecaed7e2c961609346775.

Olivares, L., Lisboa, J., Marin, J., Barrera, M., 2015. Coating of Leu foil with electrodeposited nickel for 99Mo production. 2015. Proceedings of the 2015 European Research Reactor Conference (RRFM) held in Bucharest, Romania on 19-23 April, 2015. European Nuclear Society. Brussels, Belgium, 2015. pp. 370. (available at: https://inis.iaea.org/collection/NCLCollectionStore/_Public/47/116/47116398.pdf?r=1.

Perrotta, J.A., Obadia, I.J., 2011. The RMB Project development status. In: Proceeding of International Conference on Research Reactors: Safe Management and Effective Utilization. Session C: New Research Reactor Projects. 14-18 November 2011, Rabat, Morocco. Proceedings series. International Atomic Energy Agency. 2012. STI/PUB/1575 978-92-0-184610-5 (available at: https://www-pub.iaea.org/MTCD/Publications/PDF/P1575_CD_web/datasets/abstracts/C6Perrotta.html.

Perrotta, J.A., Soares, A.J., 2014. RMB: The new Brazilian Multipurpose Research Reactor. In: International Topical Meeting on Research Reactor Fuel Management RRFM 2014, Ljubljana, Slovenia, 20 March – 3 April, P. 394-401, 2014 (available at: https://www.euronuclear.org/download/proceedings-rrfm-2014/.

Ponsard, B., 2010. Mo-99 supply issues: status report and lessons learned. In: International Topical Meeting on Research Reactor Fuel Management RRFM 2010, Marrakech, Morocco, 21-25 March, 2010 (available at: https://www.euronuclear.org/download/proceedings-rrfm-2010/?wpdmdl=3046&refresh=5fecaed7e2c961609346775.

Ryu, H.J., Kim, C.K., Sim, M.S., Park, J.M., Lee, J.H., 2013. Development of high-density U/Al dispersion plates for Mo-99 production using atomized uranium powder. Nucl. Eng. Technol. 45, 979–986. https://doi.org/10.5516/NET.07.2013.014.

Solbrekken, G.L., Turner, K., Allen, C., 2009. Engineering of LEU-foil based Mo-99 target for high volume production. In: Proceeding of International Meeting on Reduced Enrichment for Research and Test Reactors, Beijing, China, 1-5 November, 2009 (available at: https://www.rertr.anl.gov/RERTR31/pdf/S12-P1_Solbrekken.pdf.

Vandegrift, G.F, Snelgrove, J.L., Aase, S., Bretscher, M.M., Buchhoh, B.A., Chaiko, D.J., Chamberlain, D.B., Chen, L., Conner, C., Dong, D., Hofman, G.L., Hutter, J.C., Knighton, G.C., Kwok, I.D., Leonard, R.A., Matos, J.E., Sedlet, J., Srinivasan, B., Walker, D.E., Wiencek, T., Wood, E.L., Wygmans, D. G., Travelli, A., Landsberger, S., Wu, D., Suripto, A., Mutalib, A., Nasution, H., Adang, H.G., Hotman, L., Almini, S., Dedi, S., Martalena, R., Gogo, A., Purwadi, B., Amin, D.L., Zahiruddin, A., Sukmana, Kadarisman, Sriyono, Hafid, D., Sayadet, M., 1999. Converting Targets and Processes for Fission-Product 99Mo from High to Low-Enriched Uranium. Production technologies for molybdenum-99 and technetium-99m. International Atomic Energy Agency, Vienna, Austria, 1999. IAEA-TECDOC-1065 (available at: https://inis.iaea.org/collection/NCLCollectionStore/_Public/30/013/30013596.pdf?r=1&r=1.

Vandegrift, G., Brown, M.A., Jerden, J.L., Gelis, A.V., Stepinski, D.C., Wiedmeyer, S., Youker, A., Hebden, A., Solbrekken, G., Allen, C., Robertson, D., El-Gizawy, S., Govindarajan, S., Hoyer, A., Makarewics, P., Harris, J., Graybill, B., Gunn, A., Berlin, J., Bryan, C., Sherman, S., Hobbs, R., Griffin, F., Carbajo, J., Freels, J., Chandier, D., Hurt, C.J., Williams, P., 2016. Low-Enriched Uranium High-Density Target Project: Compendium Report, ANL/NE-16/15, Argonne National Laboratory, September, 2016 (available at: https://publications.anl.gov/anlpubs/2016/11/130420.pdf.

Verbeek, P., 2008. Report on Molybdenum 99 production for nuclear medicine 2010-2020, Association of Imaging Producers & Equipment Suppliers. (available at: https://www.oecd-nea.org/med-radio/docs/200902_AIPESMolySupplyReport.pdf.

Wiencek, T. C.; Hofman, G. L., 1993. Development of Uranium Metal Targets for 99Mo Production. Proceedings of the 1993 International Meeting on Reduced Enrichment for Research and Test Reactors (RERTR) held in Oarai, Japan on October 4-7, 1993. Japan Atomic Energy Research Institute, March 1994, p. 385. JAERI –M 94-042 (available at: https://www.osti.gov/servlets/purl/10189292.

Wiencek, T.C., Vandergrift, G.F., Bakel, A., Leyva, A.A., Hebden, A.S., 2008. Status and progress of foil and target fabrication activities for the production of 99Mo from LEU. Proceeding of International Meeting on Reduced Enrichment for Research and Test Reactors.

Wiencek, T.C., Vandegrift, G.F., Bakel, A., 2009. Conceptual Process and Facility Design to Produce Low-Enriched Uranium Targets for the Production of 99Mo Medical Radioisotopes, ANL/CSE-13/32, Argonne National Laboratory, January, 2009 (available at: *77307.pdf (anl.gov).